Multiscale Computational Study of Perovskite Materials Using Classical Molecular Dynamics and Ab Initio Approaches

Noelia Faginas-Lago[1,2,3(✉)], Luca Mancini[1,2], Andrea Lombardi[1,2,3], Amanda Covarelli[2,3], Bernardino Tirri[4], and Filippo De Angelis[1,2,3]

[1] Dipartimento di Chimica, Biologia e Biotecnologie, Università degli Studi di Perugia, 06123 Perugia, Italy
[2] Dipartimento di Ingegneria Civile ed Ambientale, Università degli Studi di Perugia, 06125 Perugia, Italy
noelia.faginaslago@unipg.it
[3] Istituto CNR di Scienze e Tecnologie Chimiche "Giulio Natta" (CNR-SCITEC), 06123 Perugia, Italy
[4] Eni S.p.A, Via Emilia 1, 20097 San Donato Milanese (Milan), Italy

Abstract. In recent years, perovskite materials have emerged as promising candidates for applications in photovoltaics and photocatalysis due to their remarkable optoelectronic properties, low-cost synthesis, and structural tunability. However, their long-term stability and interactions with external molecules, such as CO_2, remain significant challenges for practical applications. In this work, we combine classical molecular dynamics (MD) simulations and ab initio calculations to investigate the structural, electronic, and dynamical properties of perovskite materials. Density Functional Theory (DFT) calculations are employed to optimize the atomic geometries and determine charge distributions, while MD simulations provide insights into the system behavior under different thermodynamic conditions. Particular attention is given to the preliminary analysis of non-covalent interactions between perovskite structures and CO_2 molecules, modeled using the canonical LennardJones potential. The results highlight the balance between long-range attractive and short-range repulsive forces governing these interactions and contribute to a more accurate description of intermolecular potentials. This study provides a basis for the development of improved force fields and enhances the predictive capability of computational models for perovskite-based systems in energy and environmental applications. These findings may support future efforts to optimize perovskite materials for sustainable energy conversion and CO_2 reduction technologies.

Keywords: Perovskite · Molecular Dynamics · Ab Initio Calculations · Density Functional Theory · Non-Covalent Interactions · Photovoltaics · CO_2 Reduction · Force Field Development

© The Author(s), under exclusive license to Springer Nature Switzerland AG 2027
O. Gervasi et al. (Eds.): ICCSA 2026 Workshops, LNCS 16765, pp. 212–224, 2027.
https://doi.org/10.1007/978-3-032-30536-7_14

1 Introduction

Perovskite, originally considered the mineral name of calcium titanate ($CaTiO_3$) [1], was discovered for the first time by Russian mineralogist Lev Perovskij. Perovskites are used in photovoltaics because of their increasing power conversion efficiency (PCE), low-cost materials constituents, simple solution fabrication process [2], high absorption coefficient in a wide wavelength range and relatively high carrier mobility of free electrons and holes [1]. Initiated in 2009 with an efficiency of 3.8% [2], Perovskite solar cells (PSCs) have now achieved a lab-scale power conversion efficiency of 26.7% [3], competing with the performance of commercial silicon solar cells. Perovskites have a general chemical formula of ABX_3, where A is usually an organic cation such as methylammonium (MA) or formamidinium (FA), B is a metallic cation like tin or lead and X is an halide, such as I, Br or Cl [4]. The A-site cation is coordinated to 12 X anions, forming a cuboctahedron, while the 6-fold-coordinated B-site cation has an octahedral geometry [1], as shown in Fig. 1.

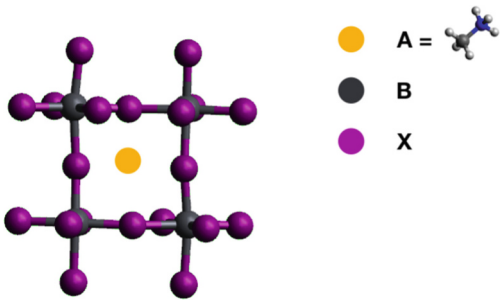

Fig. 1. A 3D molecular structure shows a cubic arrangement of atoms connected by bonds. Three types of atoms are indicated by colored circles: orange for type A, dark gray for type B, and purple for type X. The structure highlights how these atoms are positioned relative to each other, with type B atoms at the cube corners and type X atoms along the edges.

Perovskite solar cells (PSCs) are typically characterized by a layered device architecture consisting of a transparent conductive oxide (TCO)-coated glass substrate, an n-type semiconductor acting as the electron transport layer (ETL), a perovskite absorber layer, a p-type semiconductor serving as the hole transport layer (HTL), and a back contact made of metal, TCO, or carbon [2]. Despite their remarkable optoelectronic properties and high efficiency, the large-scale commercialization of perovskite-based devices is still hindered by their limited stability. The main factors contributing to degradation are moisture, ultraviolet (UV) radiation, and elevated temperatures [5].

The irreversible degradation of the perovskite absorber critically affects the operational lifetime of photovoltaic devices. In particular, exposure to UV light

has been shown to reduce the charge collection efficiency even in encapsulated cells, as demonstrated by transient absorption spectroscopy (TAS) studies [5]. Thermal instability represents another major issue: elevated temperatures can induce significant structural and chemical changes in perovskite materials. For instance, Phillippe et al. [6] investigated the thermal degradation of $MAPbI_3$ and $MAPbI_3$ - xClx films using hard X-ray photoelectron spectroscopy (XPS), which allows for compositional analysis independent of crystallinity. Their experiments, conducted under ultra-high vacuum to isolate temperature effects, revealed that increasing temperature leads to a progressive decrease in the I/Pb and N/Pb ratios, indicating decomposition into PbI_2. Specifically, heating at 100 ^{circ}C for 20 min caused a noticeable reduction in both ratios, while treatment at 200 ^{circ}C resulted in complete conversion to PbI_2.

To address these stability challenges, several strategies have been proposed, including compositional engineering, morphology control, grain size optimization, advanced deposition techniques, and interfacial engineering [7]. Among these, the incorporation of additives represents a simple yet effective approach, as small quantities of suitable compounds can significantly improve both material properties and device stability [7].

Beyond photovoltaics, perovskite materials have recently attracted considerable attention for applications such as water splitting and CO_2 reduction [8]. In the context of the increasing atmospheric CO_2 levels driven by anthropogenic activities [9–12], photoelectrochemical CO_2 reduction emerges as a promising strategy for carbon mitigation and the development of carbon-neutral technologies. Although numerous studies have explored the catalytic potential of perovskites for CO_2 conversion [13–18], the underlying reaction mechanisms remain not fully understood. A crucial initial step in this process is the long-range interaction between the CO_2 molecule and the perovskite surface. This interaction determines the formation of weakly bound precursor states, which in turn guide the system along specific reaction pathways. Therefore, a detailed understanding of intermolecular forces governing these early-stage interactions is essential for elucidating the overall reaction mechanism.

One of the first step of the process, which is common of all chemical processes, is represented by the long-range interaction of the CO_2 molecule with the surface of the perovskite. Such interaction will then lead to different configurations of the weakly bound precursor state of the system, which drives the species involved along specific chanels of the reactivity. Therefore, a detailed analysis of the long-range interaction and of the intermolecular forces driving the initial process can be pivotal for a better understanding of all the reactive process. In order to properly characterize the initial interaction between the two interacting species, a valid approach consists in the use of Molecular Dynamics (MD) simulations considering the appropriate range of thermodynamic conditions. As a first step, it is pivotal to implement the most accurate description of the interactions of the involved molecules through the development of a Force Field (FF), which represents a challenging task [19–21] since the choice of a correct intermolecular force field, modelling the intermolecular forces, crucially

influences the realism and feasibility of the simulation studies [21]. Different functions can be used to describe the non electrostatic component of the intermolecular interaction, including the classical Lennard-Jones potential [22], but also the more accurate *Improved Lennard-Jones* (ILJ) formulation [23], which allow for a better representation of long range attraction and short range repulsion. In the present contribution we performed preliminary MD calculation for the system composed of a perovskite layer, composed of 408 atoms in total, with 40 Pb atoms, 112 I atoms and 32 methylammonium ions ($CH_3NH_3^+$),both isolated and interacting with a CO_2 molecule using a LJ force field. The work constitutes a starting point toward the development of more accurate force field based on the physical properties of the interacting molecules.

2 Theoretical Methods

2.1 Ab Initio Calculations

Ab initio calculations have been performed at the DFT level of theory for the perovskite system. In depth, the structure of the perovskite has been optimized using the PBE functional and ultrasoft pseudopoptentials. The wavefunction and charge density cutoffs have been set to 40 Ry and 360 Ry, respectively. Long-range electron interactions have been taken into account applying the Grimme-D3 correction for the dispersion forces, which have an important role in determining the adsorption energy in large neutral molecules. The k-point sampling mesh is the Γ-mesh and a vacuum of 30 Å was added to create the slab. The same computational strategy has been adopted for the optimization of the CO_2 molecule and the system composed of a carbon dioxide molecule interacting with the perovskite slab. All calculations have been performed with the Quantum Espresso package [24–26].

As already reported in previous works [27], the main properties of the CO_2 molecule, necessary for the correct implementation of the force field, has been obtained through a DFT analysis, which represents a good compromise between chemical accuracy and computational cost [28–33].

2.2 Molecular Dynamics

Classical molecular dynamics simulations have been performed using the DL_POLY [34] simulation package, considering the NVT ensamble, where the number of particles (N), volume (V) and temperature (T) are kept constant. For this purpose, a Hoover-Nose thermostat [35] has been used, with a relaxation constant of 1 ps. Parallelepiped boundary conditions have been used considering a simulation box of 83×89 x 85 $Å^3$. All the simulations have been performed considering a temperature of 10 K and a pressure of 1 atm. An initial equilibration period of 1.5 ns has been performed, considering a total simulation time of 5 ns

Non-covalent Interactions: Potential Energy Surface. In order to obtain a reliable Force Field to be used in the simulation, the global intermolecular interaction energy (V_{Tot}) has been considered as a combination of an electrostatic contribution (V_{Elec}) and a non-electrostatic contribution (V_{Nelec}):

$$V_{Tot} = V_{Elec} + V_{Nelec} \tag{1}$$

where the electrostatic contribution has been calculated taking into account the atomic charge distribution of the CO_2 molecule, already reported in the ref. [27]. Differently than the previous treatment, the $MAPbI_3$ system has been treated considering the various functional groups constituting the Perovskite slab. Consequently, in the construction of the force field, lead was treated as Pb^{2+}, iodine as I^-, and methylammonium was represented as a single effective atom X carrying a charge +1.

The non-electrostatic component of the intermolecular interaction has been evaluated considering the *Improved Lennard-Jones* (ILJ) formulation described in ref. [23]. The ILJ potential model for a pair of neutral particles can be formulated as follows:

$$V_{nelec} = V_{ILJ} = \varepsilon \left[\frac{m}{n(r) - m} \left(\frac{r_m}{r} \right)^{n(r)} - \frac{n(r)}{n(r) - m} \left(\frac{r_m}{r} \right)^{m} \right] \tag{2}$$

where ε and r_m represents the well depth and its location, respectively, while m assumes the value of 6 for neutral-neutral systems. Finally, the term $n(r)$ is defined as:

$$n(r) = \beta + 4 \left(\frac{r}{r_m} \right)^2 \tag{3}$$

The parameters used for the ILJ formulation of the interaction are reported in Table 1

Table 1. List of the Improved Lennard-Jones parameters evaluated for the Perovskite + CO_2 system (where X indicates the $CH_3NH_3^+$ moiety).

Interacting Pair	ε (meV)	r_m (Å)
C - Pb	7.07	3.65
O - Pb	9.67	3.78
C - I	6.69	4.31
O - Pb	10.73	4.36
C - X	6.26	3.94
O - X	9.28	4.03

The value of β is usually considered in the interval between 6 and 8.

3 Results and Discussion

3.1 Ab Initio Results

An initial *ab initio* analysis was carried out (see Sect. 2 for details) considering a relaxation (optimization) procedure, where the first three layers from the bottom of the perovskite structure (along the z-axis) are kept rigid, while the last two layers, which are closer to the CO_2 molecule, are able to relax. The same strategy has been used for both the isolated perovskite and the perovskite interacting with the CO_2 molecule. The resulting structure, obtained through *ab initio* calculations, is reported in Fig. 2.

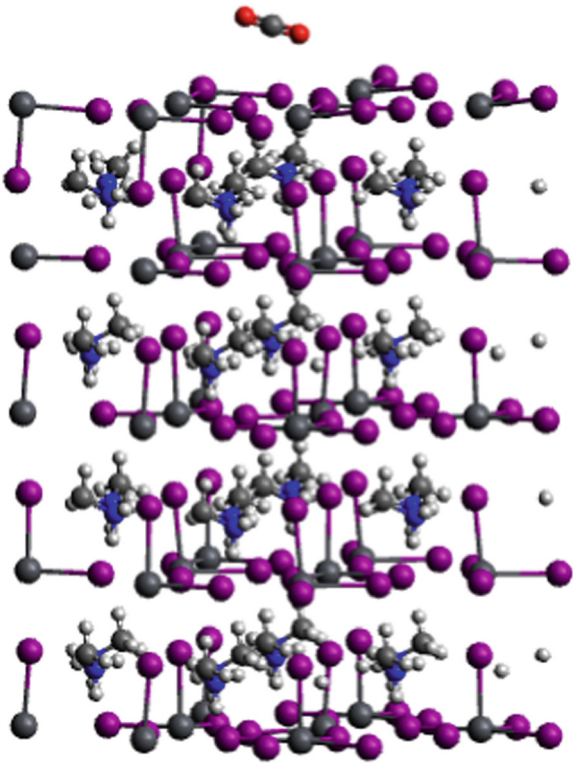

Fig. 2. 3D representation of the structure of the CO_2 molecule interacting with a perovskite system with $E_{ads} = -6.61$ kcal/mol.

The energy of the system can be easily calculated, allowing to quantify the strength of the interaction between the CO_2 molecule in the gas phase and the surface of the perovskite. In details, the adsorption energy can be evaluated as follows:

$$E_{ads} = E_{tot} - E_{per} - E_{\mathrm{CO_2}} \tag{4}$$

where E_{tot} is the energy deriving from the optimized structure of the perovskite with the CO_2 molecule, while E_{per} and E_{CO_2} represent the energies of the perovskite and CO_2 optimized separately, obtained at the DFT level of theory. Following the formulation reported in Eq. 4, a value of $E_{ads} = -6.61$ kcal/mol was obtained. This value is the result of a series of calculations where the initial geometry was modified: specifically, the CO_2 was put once above the Pb and once above the I of the slab and rotated to respect of the C atom with a step of 20^{circ}. So two series of results have been obtained and the most stable interaction has been reported. The same interaction can be evaluated without considering the Grimme-D3 dispersion correction. In this case, $E_{ads} = -6.20$ kcal/mol, with a difference of -0.41 kcal/mol. Although the difference is not very big, it is significant for a little molecule such as CO_2, suggesting that the interaction is driven by both chemical adsorption and van der Waals forces. An additional analysis can be performed considering the geometry resulting from *ab initio* calculations, and in particular taking into account the distance between the CO_2 molecule and the Perovskite layer. In Table 2 are reported the main distances obtained through accurate *ab initio* calculations.

Table 2. Atom-atom distances (in Å) between the CO_2 molecule and the first layer of the perovskite structure, with $E_{ads} = -6.61$ kcal/mol, obtained through DFT calculations (see Sect. 2.1 for details).

Interacting Pair	dist. (Å)
C - Pb	3.944
O - Pb	3.108
C - I	3.608
O - I	3.788

3.2 Classical Molecular Dynamics Results

As already reported in a previous investigation [27], the Perovskite system has been considered as composed of 408 atoms in total, organized in four layers considering a total of 40 Pb atoms, 112 I atoms and 32 methylammonium ions ($CH_3NH_3^+$). In order to run proper MD simulations, an essential step is represented by the accurate selection of an appropriate force field. As reported in previous section, a series of ILJ parameters for the main atom-atom interactions have been derived considering the $CH_3NH_3^+$ ion as an "effective" center (indicated as "X"), carrying the global charge and polarizability of the whole cation. Electrostatic contributions has been taken into account considering a three-center model for CO_2 [27], where the charges for each atom have been calculated at the DFT level of theory, while for the Perovskite the charges of the various functional groups have been considered. No induction therms have been included in the calculations.

An initial assessment of the simulation parameters has been performed considering the evolution of the values of temperature and configurational (potential) energy along the simulation time. In Figs. 3 and 4 are reported the trends of the configurational energy and temperature as a function of the simulation time.

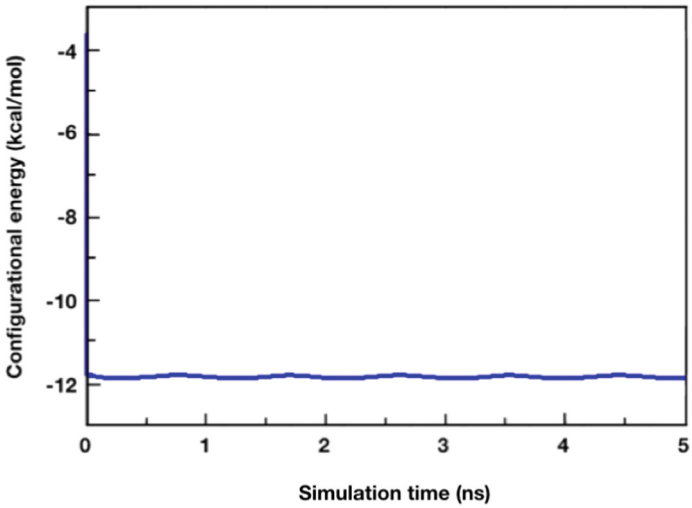

Fig. 3. Trend of the total energy (in kcal/mol) as a function of the simulation time (ns) for the Perovskite system, obtained through MD calculations.

The small fluctuations observed in energy and temperature throughout the MD simulations, relative to their absolute values, indicate that the chosen simulation parameters are reliable and well-suited for the system. Following the same protocol employed for the *ab initio* investigation of the system (see previous sectio for details), the interaction energy was evaluated considering the difference between the configurational energy of the perovskite+CO_2 system and the configurational energy of the two interacting species, calculated separately in the MD framework. The value obtained from classical MD calculation is equal to −11 kcal/mol, showing a significant deviation from the results of *ab initio* calculations. Additionally, the final configuration of the MD analysis can be compared with the geometry of the optimized system at the DFT level of theory. In Fig. 5 is reported a schematic representation of the final structure of the Perovskite-CO_2 system obtained from MD calculations

A significant parameter is represented by the distance between the CO_2 molecule and the Perovskite layer, whose values are reported in Table 3 and compared with the main distances obtained through accurate *ab initio* calculations.

The OI distance is the most representative descriptor of the adsorption geometry, as it approximates the distance between the terminal O of CO_2 and the surface of the perovskite material. A very good agreement is found between DFT

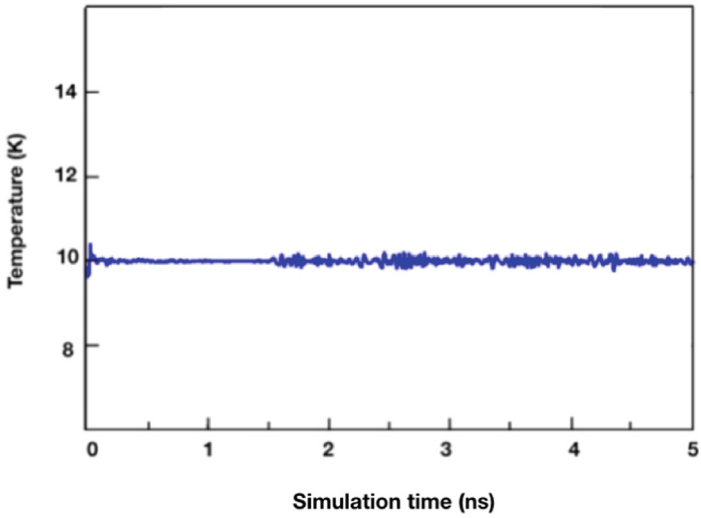

Fig. 4. Trend of the temperature (in K) as a function of the simulation time (ns) for the Perovskite system.

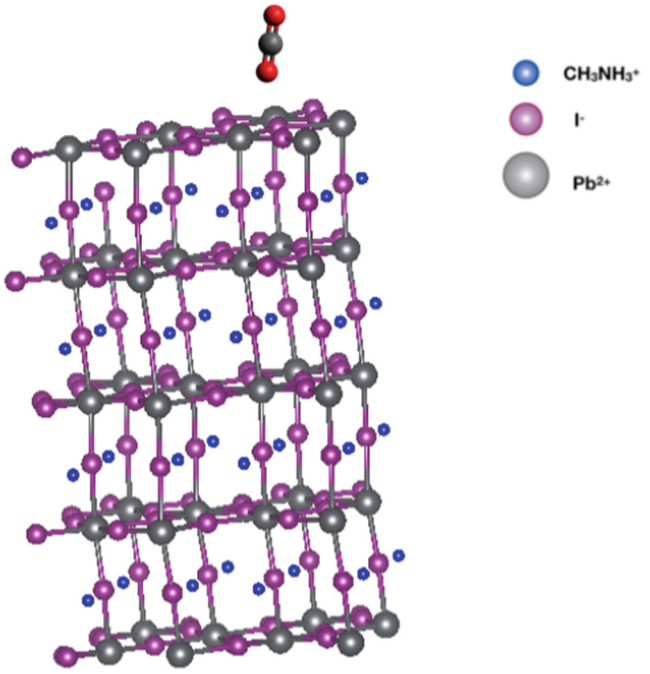

Fig. 5. Schematic representation of the final structure of the Perovskite-CO_2 system obtained from MD calculations.

Table 3. Atom-atom distances (in Å) between the CO_2 molecule and the first layer of the perovskite structure, through DFT and MD calculations.

Interacting Pair	dist. (Å) *DFT*	dist. (Å) *MD*
C- Pb	3.94	5.54
O - Pb	3.11	4.67
C - I	3.61	4.95
O - I	3.79	3.93

(3.79 Å) and MD (3.93 Å), confirming that the classical model correctly reproduces the adsorption geometry. Despite the quantitative difference between the two values of energy, both approaches predict the same order of magnitude for the CO_2-perovskite interaction. Additionally, the ILJ-based classical model was specifically parameterized for this system, rather than adopting generic literature parameters, with the aim of representing polarizability effects as accurately as possible. This approach yields an adsorption geometry in close agreement with the DFT results. The remaining discrepancy in the interaction energy can be mainly attributed to the intrinsically simplified nature of the classical description, in which the methylammonium (MA) cation is treated as a single interaction center. This approximation simplifies the interaction by neglecting internal bonding contributions and reinforces the description of the perovskite as an ionic crystal, which, while computationally efficient, can lead to minor deviations with respect to the fully electronic DFT treatment. Finally, the interfacial spatial correlations between CO_2 and the perovskite surface were characterized using radial distribution functions computed from molecular dynamics trajectories. The distributions were evaluated between CO_2 carbon and oxygen atoms and surface iodide atoms by accumulating pair distances over all simulation frames. The results obtained are shown in Fig. 6

The radial distribution function (RDF) between the oxygen atom of CO_2 and iodine atoms of $MAPbI_3$ shows a primary peak around 3.76 Å, indicating the most probable distance between CO_2 molecules and the halide sites on the surface layer. Lower-intensity secondary peaks, appearing at larger distances, likely originate from interactions with the oxigen atom of the CO_2 molecule and other iodine atoms in subsurface layers, reflects contributions from the perovskite lattice below the outermost layer.

4 Conclusions

In this work, a multiscale computational approach has been employed that combines Density Functional Theory (DFT) and classical Molecular Dynamics (MD) simulations to investigate the structural and interaction properties of perovskite materials in the presence of CO_2 molecules. The study provides a preliminary but insightful analysis of the non-covalent interactions governing the adsorption process at the perovskite surface.

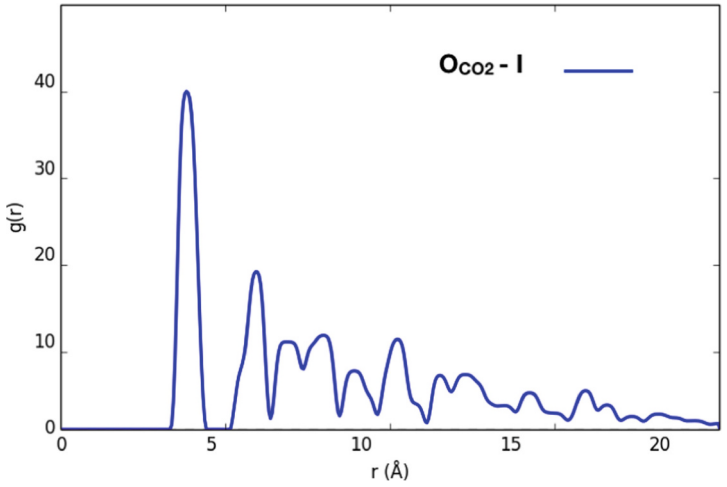

Fig. 6. Radial distribution function between CO_2 and the perovskite surface.

The DFT results reveal that CO_2 interacts weakly with the perovskite surface, with an adsorption energy of −6.61 kcal/mol, confirming the physisorption nature of the process. The optimized geometries highlight the key role of intermolecular distances, particularly involving oxygen and iodine atoms, in defining the adsorption configuration. Classical MD simulations, based on an Improved Lennard-Jones (ILJ) semi-empirical force field, specifically parameterized for this system, successfully reproduce the structural features of the adsorption process, showing good agreement with DFT results in terms of geometrical parameters. Although a discrepancy in interaction energies is observed (−11 kcal /mol from MD), this difference can be attributed to the simplified representation of the system in the classical model, particularly the treatment of the methylammonium cation as a single interaction center.

Overall, the combination of ab initio and classical approaches demonstrates the reliability of the developed force field in capturing the essential physics of the CO_2perovskite interaction. These findings represent a solid starting point for the development of more accurate and transferable force fields, ultimately contributing to improved predictive models. Such advancements are crucial for optimizing perovskite materials in applications related to sustainable energy conversion and CO_2 reduction technologies.

Acknowledgments. L. M. acknowledges the European Union - NextGenerationEU under the Italian Ministry of University and Research (MUR) National Innovation Ecosystem grant ECS00000041 - VITALITY - CUP J97G22000170005. N.F.L acknowledges funding by Mission 4, Component 2, Investment 1.1, Call for tender No. 104 published on 2.2.2022 by the Italian Ministry of University and Research (MUR), funded by the European Union NextGenerationEU Project Title 2022JC2Y93 ChemicalOrigins: linking the fossil composition of the Solar System with the chemistry of protoplanetary disks CUP J53D23001600006 - Grant Assignment Decree No. 962 adopted on 30.06.2023 by the Italian Ministry of Ministry of University and Research (MUR). F. D, N. F. L and A. L acknowledge funding by the Italian Ministry of Environment and

Energy Security in the framework of the Project GoPV (CSEAA_00011) for Research on the Electric System. A.C., from UniPG, acknowledges the financial support of Eni S.p.A. for research activities conducted within the PhD cycle XXXIX.

Disclosure of Interests. The authors have no competing interests to declare that are relevant to the content of this article.

References

1. Kim, J.Y., Lee, J.W., Jung, H.S., Shin, H., Park, N.G.: High-efficiency perovskite solar cells. Chem. Rev. **120**(15), 7867–7918 (2020)
2. Rong, Y., et al.: Challenges for commercializing perovskite solar cells. Science **361**(6408), eaat8235 (2018)
3. Mao, L., Xiang, C.: A comprehensive review of machine learning applications in perovskite solar cells: materials discovery, device performance, process optimization and systems integration. Mater. Today Energy, 101742 (2024)
4. Correa-Baena, J.P., et al.: Promises and challenges of perovskite solar cells. Science **358**(6364), 739–744 (2017)
5. Wang, D., Wright, M., Elumalai, N.K., Uddin, A.: Stability of perovskite solar cells. Sol. Energy Mater. Sol. Cells **147**, 255–275 (2016)
6. Philippe, B., et al.: Chemical and electronic structure characterization of lead halide perovskites and stability behavior under different exposures? a photoelectron spectroscopy investigation. Chem. Mater. **27**(5), 1720–1731 (2015)
7. Valero, S., Soria, T., Marinova, N., Delgado, J.L.: Efficient and stable perovskite solar cells based on perfluorinated polymers. Polym. Chem. **10**(42), 5726–5736 (2019)
8. Bienkowski, K., et al.: Halide perovskites for photoelectrochemical water splitting and co2 reduction: challenges and opportunities. ACS Catal. **14**(9), 6603–6622 (2024)
9. Harfoot, M.B., et al.: Present and future biodiversity risks from fossil fuel exploitation. Conserv. Lett. **11**(4), e12448 (2018)
10. Deutz, S., et al.: Cleaner production of cleaner fuels: wind-to-wheel-environmental assessment of co_2-based oxymethylene ether as a drop-in fuel. Energy Environ. Sci. **11**(2), 331–343 (2018)
11. Marques, A.C., Fuinhas, J.A., Pereira, D.A.: Have fossil fuels been substituted by renewables? An empirical assessment for 10 European countries. Energy Policy **116**, 257–265 (2018)
12. Rogelj, J., et al.: Scenarios towards limiting global mean temperature increase below 1.5 c. Nat. Clim. Chang. **8**(4), 325–332 (2018)
13. Tang, C., Chen, C., Xu, W., Xu, L.: Design of doped cesium lead halide perovskite as a photo-catalytic co 2 reduction catalyst. J. Mater. Chem. A **7**(12), 6911–6919 (2019)
14. Shyamal, S., Pradhan, N.: Halide perovskite nanocrystal photocatalysts for co2 reduction: successes and challenges. J. Phys. Chem. Lett. **11**(16), 6921–6934 (2020)
15. Chen, J., Dong, C., Idriss, H., Mohammed, O.F., Bakr, O.M.: Metal halide perovskites for solar-to-chemical fuel conversion. Adv. Energy Mater. **10**(13), 1902433 (2020)
16. Zhang, X., Tang, R., Li, F., Zheng, R., Huang, J.: Tailoring inorganic halide perovskite photocatalysts toward carbon dioxide reduction. Solar RRL **6**(6), 2101058 (2022)

17. Yuan, J., Liu, H., Wang, S., Li, X.: How to apply metal halide perovskites to photocatalysis: challenges and development. Nanoscale **13**(23), 10281–10304 (2021)
18. Chen, S., Yin, H., Liu, P., Wang, Y., Zhao, H.: Stabilization and performance enhancement strategies for halide perovskite photocatalysts. Adv. Mater. **35**(6), 2203836 (2023)
19. Marques, J., et al.: A global optimization perspective on molecular clusters. Philos. Trans. R. Soc. A Math. Phys. Eng. Sci. **375**(2092), 20160198 (2017)
20. Cappelletti, D., Falcinelli, S., Pirani, F.: The dawn of hydrogen and halogen bonds and their crucial role in collisional processes probing long-range intermolecular interactions. Phys. Chem. Chem. Phys. **26**, 7971–7987 (2024)
21. Marques, J.M., Prudente, F.V., Pirani, F.: Intermolecular forces: from atoms and molecules to nanostructures (2022)
22. Lennard-Jones, J., Hall, G.: Je lennard-jones proc. Roy. Soc. Lond. A. **106**, 441 (1924)
23. Pirani, F., Brizi, S., Roncaratti, L.F., Casavecchia, P., Cappelletti, D., Vecchiocattivi, F.: Beyond the lennard-jones model: a simple and accurate potential function probed by high resolution scattering data useful for molecular dynamics simulations. Phys. Chem. Chem. Phys. **10**(36), 5489–5503 (2008)
24. Giannozzi, P., et al.: Quantum espresso: a modular and open-source software project for quantum simulations of materials. Journal of Physics: Condensed Matter **21**(39), 395502 (19pp) (2009). http://www.quantum-espresso.org
25. Giannozzi, P., et al.: Advanced capabilities for materials modelling with quantum espresso. J. Phys. Condens. Matter. **29**(46), 465901 (2017). http://stacks.iop.org/0953-8984/29/i=46/a=465901
26. Giannozzi, P., et al.: Quantum espresso toward the exascale. J. Chem. Phys. **152**(15), 154105 (2020)
27. Faginas-Lago, N., et al.: Computational insights into perovskite materials: classical molecular dynamics and ab initio approaches. In: International Conference on Computational Science and Its Applications, pp. 3–16. Springer, Cham (2025)
28. Liang, P., et al.: Oh (2π)+ c2h4 reaction: a combined crossed molecular beam and theoretical study. J. Phys. Chem. A **127**(21), 4609–4623 (2023)
29. Rosi, M., et al.: Electronic structure and kinetics calculations for the si+ sh reaction, a possible route of sis formation in star-forming regions. In: Computational Science and Its Applications–ICCSA 2019: 19th International Conference, Saint Petersburg, Russia, July 1–4, 2019, Proceedings, Part III 19, pp. 306–315. Springer, Cham (2019)
30. Mancini, L., et al.: A computational characterization of the reaction mechanisms for the reactions n (2d)+ ch3cn and hc3n and implications for the nitrogen-rich organic chemistry of titan. Comput. Theor. Chem. **1229**, 114341 (2023)
31. Mancini, L., et al.: Destruction of interstellar methyl cyanide (ch3cn) via collisions with he+? ions. Astron. Astrophys. **691**, A83 (2024)
32. Richardson, V., et al.: Fragmentation of interstellar methanol by collisions with he+: an experimental and computational study. Phys. Chem. Chem. Phys. **24**(37), 22437–22452 (2022)
33. Valença Ferreira de Aragão, E., Mancini, L., Faginas-Lago, N., Rosi, M., Skouteris, D., Pirani, F.: Semiempirical potential in kinetics calculations on the hc3n+ CN reaction. Molecules **27**(7), 2297 (2022)
34. Smith, W., Yong, C., Rodger, P.: Dl_poly: application to molecular simulation. Mol. Simul. **28**(5), 385–471 (2002)
35. Hoover, W.G.: Canonical dynamics: equilibrium phase-space distributions. Phys. Rev. A **31**(3), 1695 (1985)